Author Manuscript

Author Manuscript

Author Manuscript

Author Manuscript

HHS Public Access

Author manuscript

Cortex. Author manuscript; available in PMC 2015 August 01.

Published in final edited form as:

Cortex. 2014 August ; 57: 167–176. doi:10.1016/j.cortex.2014.04.006.

Aberrant functional connectivity in Papez circuit correlates with memory performance in cognitively intact middle-aged *APOE4* carriers

Wenjun Li, PhD[1,†], **Piero G. Antuono, MD**[2,†,††], **Chunming Xie, MD, PhD**[1], **Gang Chen, PhD**[1], **Jennifer L. Jones, MS**[2], **B. Douglas Ward, MS**[1], **Suraj P. Singh, MD**[2], **Malgorzata B. Franczak, MD**[2], **Joseph S. Goveas, MD**[3], and **Shi-Jiang Li, PhD**[1,3,††]

[1]Department of Biophysics, Medical College of Wisconsin, Milwaukee, WI USA

[2]Department of Neurology, Medical College of Wisconsin, Milwaukee, WI USA

[3]Department of Psychiatry and Behavioral Medicine, Medical College of Wisconsin, [†]Milwaukee, WI USA

Abstract

The main objective of this study is to detect the early changes in resting-state Papez circuit functional connectivity using the hippocampus as the seed, and to determine the associations between altered functional connectivity (FC) and the episodic memory performance in cognitively intact middle-aged APOE4 carriers who are at risk of Alzheimer's disease (AD). Forty-six cognitively intact, middle-aged participants, including 20 APOE4 carriers and 26 age-, sex-, and education-matched noncarriers were studied. The resting-state FC of the hippocampus (HFC) was compared between APOE4 carriers and noncarriers. APOE4 carriers showed significantly decreased FC in brain areas that involve learning and memory functions, including the frontal, cingulate, thalamus and basal ganglia regions. Multiple linear regression analysis showed significant correlations between HFC and the episodic memory performance. Conjunction analysis between neural correlates of memory and altered HFC showed the overlapping regions, especially the subcortical regions such as thalamus, caudate nucleus, and cingulate cortices involved in the Papez circuit. Thus, changes in connectivity in the Papez circuit may be used as an early risk detection for AD.

© 2014 Published by Elsevier Ltd.

[††]Cocorresponding Authors: Shi-Jiang Li, PhD, Department of Biophysics, Medical College of Wisconsin, 8701 Watertown Plank Road, Milwaukee, WI 53226, USA. Tel: 414-456-4029, Fax: 414-456-6512, sjli@mcw.edu; Piero Antuono, M.D., Department of Neurology, Medical College of Wisconsin, 9200 W. Wisconsin Ave., Milwaukee, WI 53226 USA, Tel: 414-805-5224, Fax: 414-456-6512, pantuono@mcw.edu.

[†]Wenjun Li, PhD, and Piero G. Antuono, MD, contributed equally to the article.

Publisher's Disclaimer: This is a PDF file of an unedited manuscript that has been accepted for publication. As a service to our customers we are providing this early version of the manuscript. The manuscript will undergo copyediting, typesetting, and review of the resulting proof before it is published in its final citable form. Please note that during the production process errors may be discovered which could affect the content, and all legal disclaimers that apply to the journal pertain.

Author Manuscript Author Manuscript Author Manuscript Author Manuscript

Keywords

Apolipoprotein E ε4; APOE4; Alzheimer's disease; resting-state functional connectivity; memory network; hippocampus; thalamus; caudate nucleus; Papez circuit

1. Introduction

Pathological features of Alzheimer's disease (AD), such as neuronal dysfunction and degeneration, invade the Papez circuitry of the medial temporal lobe (Allen et al., 2007; Greicius et al., 2004; Hornberger et al., 2012; Li et al., 2002; Madsen et al., 2010; Smith, 2002; Wang et al., 2006). The Papez circuit, which includes the hippocampus, entorhinal cortex, mammillary body, anterior thalamic nuclei, cingulate cortices and parahippocampal gyrus, is a core pathway of the limbic system involved in the formation and consolidation of the episodic memory (Callen et al., 2001; Jicha and Carr, 2010; Papez, 1937). In the early course of AD, lesions of brain regions associated with the Papez circuit, where disruptions to information processing occur, have been reported (Jones et al., 2006; Pievani et al., 2011; Zarei et al., 2010). Such damages presumably contribute to behavior impairments including deficits in episodic memory and delayed memory (Aggleton and Brown, 1999; Haase et al., 2011; Jacobs et al., 1995; Machulda et al., 2009; Welsh et al., 1991). Specifically, recent studies have investigated structural degeneration patterns in subregions of the Papez circuit in AD patients (Hornberger et al., 2012; Jicha and Carr, 2010) and white matter diffusivity changes within the subcortical structures, such as the thalamus and caudate nucleus, during the presymptomatic and symptomatic stages of familial AD (Ryan et al., 2013). However, few studies have reported whether the observed changes in the Papez circuit are the representation of the endophynotype of the epsilon 4 (ε4) allele of the human apolipoprotein E (*APOE4*) gene.

The *APOE4* is a major susceptibility gene for late-onset AD (Corder et al., 1993; Verghese et al., 2011) that also lowers the age of AD onset in its carriers (Meyer et al., 1998). Several studies have found that *APOE4* is linked to gray matter loss, decreased cerebral metabolism and alterations in neuropsychiatric task-induced BOLD activation in the hippocampus and brain regions associated with the Papez memory circuit of asymptomatic middle-aged and elderly carriers (Adamson et al., 2011; Bookheimer et al., 2000; Crivello et al., 2010; Lind et al., 2006; Small et al., 2000). Using resting-state functional connectivity MRI (R-fMRI) methods and imaging genetic approaches, several studies demonstrated the intrinsic effects of the ε4 allele on the functional architecture of the brain in the default mode network (DMN) (Filippini et al., 2009; Fleisher et al., 2009; Sheline et al., 2010a; Westlye et al., 2011). Despite aforementioned advancements, these studies focus on the DMN. The manner in which an *APOE4* status influences resting-state functional connectivity patterns in the Papez circuit in middle-aged, cognitively intact people is not well known. Such a study would provide insight in terms of understanding the early changes in the memory network. It also would have an impact on the early detection, diagnosis and increased effectiveness of treatment through preclinical intervention (Scarmeas and Stern, 2006).

Author Manuscript Author Manuscript Author Manuscript Author Manuscript

In the present study, our goal was to reveal the *APOE4* effects on functional connectivity in the Papez circuit in cognitively intact, middle-aged *APOE4* carriers and noncarriers using the hippocampus-seeded R-fMRI method (Goveas et al., 2011). We demonstrated that the functional connectivity in the Papez circuit is disrupted prior to measurable cognitive impairment in *APOE4* carriers. We also indicated that the functional connectivity in the Papez circuit brain is significantly correlated with episodic memory performance.

2. Materials and Methods

2.1 Participants

Forty-eight cognitively healthy, middle-aged participants between the ages of 44 and 65, who were caregivers or informants, accompanied patients with a diagnosis of Alzheimer's disease, were recruited through Memory Disorders Clinic of the Dementia Research Center at Medical College of Wisconsin. All participants underwent baseline neuropsychological and neurological evaluations. Laboratory tests included APOE genotyping. None of the participants had any memory complaints. Exclusion criteria included history of neurological disease; seizures or head injury with loss of consciousness within the past five years; stroke or transient ischemic attack within the past two years; drug or alcohol abuse within the past five years; major psychiatric diagnoses, including schizophrenia, mood disorders, and other neuropsychiatric disorders. Two noncarriers were excluded from the study because of incomplete scans and excessive motion during fMRI scans. The remaining 46 participants (15 males) were separated into two subject groups (Table 1) of either carriers or noncarriers of the APOE4 gene, and were enrolled for data analysis.

2.2 APOE testing

All participants provided a DNA sample for *APOE* genotype analysis. The samples were collected by buccal swab, coded and analyzed for the presence of the *APOE*2, *APOE3* and *APOE4* alleles. The material obtained was pooled. DNA was extracted in the Medical College of Wisconsin (MCW) Translational Research Units (TRUs) of the Clinical and Translational Science Institute (CTSI), using the Gentra Systems Autopure LS DNA processing system. Extracted DNA was shipped to the General Clinical Research Center (GCRC) Core Laboratory at Oregon Health and Science University for amplification. The *APOE* genotype was characterized with an analysis, which incorporated restriction-fragment-length polymorphism (Mayeux et al., 1998). The *APOE* genotype was characterized with an analysis, which incorporated restriction-fragment-length polymorphism (Mayeux et al., 1998). Sixteen of the 20 *APOE4* carriers were ε3/ε4 heterozygotes and four were ε4/ε4 homozygotes. Twentytwo of the 24 *APOE4* noncarriers are ε3/ε3 homozygotes and two are ε2/ε3 heterozygotes. The proportion of ε4 carriers in our study is higher than the general population, but is in line with the similar studies published recently (Caselli et al., 2011; Reiter et al., 2012).

2.3 Neuropsychological testing

Each participant completed a battery of neuropsychological tests at the MCW Memory Disorders Clinic. These included the Rey Auditory Verbal Learning Test for Delayed Recall (RAVLT-DR), the Boston Naming Test, the Trail Making Test (Trails-A and Trails-B),

Author Manuscript Author Manuscript Author Manuscript Author Manuscript

Digit Span, Hachinski Cerebral Ischemic Scale and the Beck Depression Inventory. Complete neuropsychological testing and physical examinations were performed. Two behavioral neurologists reviewed the medical, neurological, functional and neuropsychological data and consensus diagnoses were reached. All behavior data were analyzed with SPSS 16.0 software (http://www.spss.com, Chicago, IL.). Demographic and clinical characteristics were documented by using counts for categorical variables, means ± SD for continuous variables. Comparative analyses with independent sample *t*-tests were performed in different groups. χ^2 test was used to test the gender differences between groups.

2.4 MRI data acquisition

MRI scans were performed on a GE 3T Signa LX scanner (Waukesha, WI.) with a standard transmit and receive head coil. A high-order shimming protocol was used on each study subject to improve the field homogeneity and reduce image distortion. No specific cognitive tasks were performed and the study participants were instructed to close their eyes, relax and stay awake during the scans. R-fMRI of the whole brain was acquired in sagittal view with a single-shot gradient recalled echo-echo planer imaging pulse sequence. The parameters for R-fMRI were: TR = 2000 ms, TE = 25 ms, field of view = 24 × 24 cm^2, matrix size = 64 × 64, voxel size = 3.75 × 3.75 ×4 mm^3 and number of slices = 36. High-resolution anatomical images were acquired using 3D spoiled gradient-echo sequence for drawing the ROI and VBM analysis. The parameters were: TR = 10 ms, TE = 4 ms, TI = 450 ms, flip angle = 12°, Matrix size = 256 × 192, voxel size = 0.938 × 0.938 × 1 mm^3, and continuous 144 axial slices with 1-mm thickness.

2.5 Structural MRI data analysis

To examine whether the gray matter volume (GMV) is different between *APOE4* carriers and noncarriers, optimized voxel-based morphometry was performed, using the VBM8 toolbox in SPM (http://www.fil.ion.ucl.ac.uk/spm). First, T1-weighted images from all participants were normalized into standard space based on a group-specific gray matter template, and then segmented into white matter (WM), cerebral spinal fluid (CSF), and GMV (modulated images) (Mechelli et al., 2005). Next, the volume images were smoothed with an 8-mm Gaussian kernel followed by *logit*-transformation to make the data more normally distributed. The between-group *t*-test was then used to compare the GMV differences between *APOE4* carrier and noncarrier groups. Although familywise error (FWE) is a common technique used to correct for multiple comparisons, method in the current study to correct for the multiple comparisons (voxelwise $p < 0.05$, cluster size > 17139 mm^3 for $\alpha < 0.05$).

2.6 R-fMRI data analysis

Preprocessing of the R-fMRI data analysis was carried out, using AFNI software (http://afni.nimh.nih.gov/afni) and in-house written MATLAB programs (The MathWorks, Inc., Natick, Mass.) (Chen et al., 2011). First, the outliers and the signal trend were removed (3dDespike). Motion correction was then performed by volume registration on the resting-state fMRI data (3dvolreg). A subject demonstrating excessive movement — either more

Author Manuscript Author Manuscript Author Manuscript Author Manuscript

than 1-mm translational movement or more than 1° rotational movement, or both — was excluded from further analysis. Out of the 180 points for each voxel time series, the first five points were discarded to preserve steady-state data. Detrending was carried out to remove Legendre polynomials (3dDetrend). Further, any possible contamination from the signals from WM, CSF, the six-motion parameters, and the global average signal were regressed out from each voxel time course (3dDeconvolve). The WM and CSF masks were generated during the anatomical image segmentation procedure by including the voxels classified as 99% WM or CSF to the reference tissue probability images (SPM software). Finally, a band-pass filter was applied to keep only low-frequency fluctuations within the range of 0.015 Hz and 0.1 Hz (Fox and Raichle, 2007).

To obtain the individual HFC maps, a seed-based R-fMRI method was adopted. The bilateral hippocampus was used as the seed ROI (Li et al., 2002; Xu et al., 2008). AFNI software was used to manually trace the bilateral hippocampus regions of interest (ROI) on the sagittal slices with reference to the coronal and axial slices of the highresolution T1-weighted SPGR images of individual subjects, as described previously (Rombouts et al., 2003), after being blinded to the participants' demographics and clinical characteristics. The manually traced hippocampus ROIs only included the graymatter portions of the hippocampus head, body and tail. The hippocampus white matter regions (alveus and fimbria), the atrium and temporal horn of the lateral ventricles were used as the anatomical landmarks for the ROI identification (Konrad et al., 2009). The high-resolution hippocampus tracing was then down-sampled to the same resolution as the R-fMRI data (Figure 1). Because the spatial resolutions in SPGR and EPI images were different, each EPI image voxel that had at least 70% space containing traced hippocampus voxels in the high-resolution images was included in the hippocampal ROI analysis.

The preprocessed average-voxel time course of the hippocampus ROI was then cross-correlated with the entire brain, using the Pearson Correlation Method. The Pearson correlation coefficients (*cc*) were subjected to a Fisher's *z*-Transform, $m = 0.5\, ln(1 + cc)/(1 - cc)$, which yielded variants of approximately normal distribution. Finally, the voxelwise *m*-values were spatially normalized to a standard Talairach space coordinates and smoothed with a 6-mm Gaussian kernel for statistical analysis.

Each subject's HFC map was grouped according the subject's genotype, whether he or she was an *APOE4* carrier or noncarrier. A one-sample *t*-test was applied to obtain the HFC network pattern by testing the voxelwise HFC against the null hypothesis of no connectivity. Next, a two-sample *t*-test was used to examine the group differences in the voxelwise whole-brain HFC between the carrier group and the noncarrier group. Monte Carlo Simulation (3dClustSim) was adopted to correct falsepositive findings because of multiple comparisons for within-group comparisons (voxelwise $p < 0.01$, cluster size > 1,048 mm^3 for $\alpha < 0.05$) and between-group comparisons (voxelwise $p < 0.05$, cluster size > 4,048 mm^3 for $\alpha < 0.05$). Finally, a multiple linear regression model (3dRegAna) was adopted to investigate the neural correlates of underlying memory functions on the HFC network. Specifically, cognitive measures relating to memory (RAVLT-DR) were regressed with the voxelwise wholebrain HFC of all participants while controlling any confounding effects from age, gender, group and GMV. The voxelwise multiple linear regression maps were generated

Author Manuscript Author Manuscript Author Manuscript Author Manuscript

after correcting for multiple comparisons for voxelwise $p < 0.05$, and cluster size > 4,048 mm^3 for $\alpha < 0.05$. Conjunction analysis was used to show the overlapping brain regions between the neural correlates of the memory function and the changes in HFC. Numerical presentation was obtained by averaging the functional connectivity over the overlapping regions.

3. Results

3.1 Demographics and neuropsychological characteristics

Forty-six cognitively intact, middle-aged participants were included in the analysis. There were no significant ($p > 0.05$) differences in age, gender, education and cognitive evaluations between the two subject groups, including 20 *APOE4* carriers and 26 noncarriers (Table 1). A trend of lower RAVLT-DR ($p = 0.1$) and Digit Span ($p = 0.07$) scores was found in the *APOE4* carrier group.

3.2 Structural MRI and hippocampus ROI data

No significant differences in voxelwise whole-brain gray matter volume were found between the *APOE4* carriers and noncarriers. The mean and standard deviation of volumes of the traced hippocampus ROIs for APOE4 carriers and noncarriers were 5.25 ± 1.30 mL and 4.92 ± 1.02 mL, respectively. No significant difference was found between the two groups ($p = 0.34$).

3.3 R-fMRI data

A one-sample *t*-test was used to obtain the HFC network patterns for *APOE4* noncarriers (Figure 2, left) and carriers (Figure 2, right), respectively, for each group against zero (voxelwise $p < 0.01$, corrected cluster size > 1,048 mm^3 for $\alpha < 0.05$). In the *APOE4* noncarrier group, the hippocampus was positively correlated with brain regions including the bilateral middle temporal gyrus (MTG), parahippocampal gyrus (PHG), fusiform, amygdala, thalamus, caudate, paracentral lobule (PCL), medial frontal gyrus (MeFG), anterior cingulate cortex (ACC) and posterior cingulate cortex (PCC). The hippocampus was negatively correlated with the bilateral inferior parietal cortex (IPC) and dorsolateral prefrontal cortex (DLPFC). In the *APOE4* carrier group, the hippocampus was positively correlated only with the bilateral PCL, MTG and MeFG, ACC and PCC. The hippocampus was negatively correlated with the bilateral DLPFC and IPC.

A two-sample *t*-test was used to examine the group differences in the HFC between *APOE4* carriers and noncarriers (Figure 3). When compared to noncarriers, *APOE4* carriers showed significantly decreased HFC (voxelwise $p < 0.05$, corrected cluster size > 4048 mm^3 for $\alpha < 0.05$) in the bilateral caudate, thalamus, PCC, superior frontal gyrus (SFG), left lentiform nucleus, MeFG, inferior frontal gyrus (IFG), insula, right anterior cingulate cortex (ACC) and culmen of cerebellum (Table 2). No significantly increased HFC in carriers was found.

Multiple linear regression identified the neural correlates of underlying memory (RAVLT-DR) function on the HFC network while regressing out group, age, gender, education and GMV as covariates (voxelwise $p < 0.05$, corrected cluster size > 4,048 mm^3 for $\alpha < 0.05$).

Author Manuscript Author Manuscript Author Manuscript Author Manuscript

RAVLT-DR scores were positively correlated with HFC in the bilateral caudate, thalamus, lentiform nucleus, MeFG, ACC, culmen, right DLPFC and MTG. They were negatively correlated in the left MTG and SFG (Figure 4). Finally, conjunction analysis revealed overlapping brain regions between the neural correlates of memory performance and the decreased HFC. These brain regions include the bilateral DLPFC, caudate, thalamus and right ACC (Figure 5).

4. Discussion

The current study shows several new experimental findings that distinguish *APOE4* carriers from noncarriers, despite the fact that all participants were cognitively intact. First, we demonstrated that the HFC is significantly decreased in the subcortical regions such as the caudate, basal ganglia, and thalamus, as well as in cortical regions including MeFG, DLPFC, insula, ACC, and PCC in the *APOE4* carriers compared to the noncarriers (Figure 3 and Table 2). Second, multiple linear regression demonstrated significant correlations between HFC and episodic memory performance in the frontal, parietal, anterior cingulate, thalamus, and caudate regions for both *APOE4* carriers and noncarriers (Figure 4). Third, conjunction analysis revealed that the decreased HFC in the thalamus and caudate regions were positively correlated with the episodic memory functions. Therefore, the endophenotypes in the Papez circuit had clinical significance (Figure 5). Finally, compared with the abovementioned functional changes, no apparent gray matter volume loss was observed. This finding is consistent with previous observations that early hippocampal functional alterations can occur independently of gray matter volume changes (Dennis et al., 2010; Machulda et al., 2011; Westlye et al., 2011).

In contrast to previous reports on the intrinsic effects of the *APOE4* gene on the DMN (Filippini et al., 2009; Fleisher et al., 2009; Goveas et al., 2013; Sheline et al., 2010b; Westlye et al., 2011), not only did we find that the HFC in the cortical areas has similar characteristics to that of the DMN in the cortical regions, seen in our previous study (Goveas, et al., 2013), we also discovered *APOE4* gene effects on the HFC in the Papez circuit. To ensure that the changes in the functional connectivity involving the Papez circuit is specific to *APOE4* carriers compared to noncarriers, we compared the functional connectivity of two control networks (motor and visual) that were expected to show minimal differences between the two participant groups. We found no significant difference in cerebral cortex and subcortical regions of the motor network or the visual network between the two groups (Figure S1). The primary motor cortices (Left: −40, −23, 53; Right: 41, −22, 48 in Talairach coordinates) (Fox et al., 2009) and primary visual cortices (Left: −6, −79, −3; Right: 8, −79, −3 in Talairach coordinates) (Fox et al., 2009) were used as the seed ROIs to obtain the motor and visual network, respectively.

The involvement of Papez circuit in the progression of AD has been extensive in studies. Structurally and functionally, the thalamus and hippocampus are part of the Papez circuit (Papez, 1937). The hippocampus is tightly coupled to subcortical regions such as the caudate, basal ganglia, thalamus (Atallah et al., 2004; Villain et al., 2008; Zarei et al., 2010), in addition to the cortical brain regions in the DMN, such as the posterior cingulate, inferior parietal and frontal cortices (Vincent et al., 2008; Vincent et al., 2006). The localized

Author Manuscript Author Manuscript Author Manuscript Author Manuscript

atrophy has been found in the caudate and the Papez circuit in AD and MCI patients (Madsen et al., 2010; Smith, 2002; Zarei et al., 2010). In MCI patients, the functional activations of the subcortical regions, including the basal ganglia and the thalamus, also have been shown to diminish during encoding and recognition tasks (Machulda et al., 2009). Our results are in agreement with these findings. In addition, we found that the functional connectivity of the neural correlates of the memory function in the Papez circuit was significantly reduced in *APOE4* carriers. Considering that the *APOE4* carriers are middle-aged and cognitively intact, without apparent cognitive impairment or gray matter volume loss, it is suggested that the disruption of functional connections within the Papez circuit regions could be an endophenotype representing the AD risk. We further hypothesized that functional connectivity changes in the Papez circuit may contribute to the risk for late onset of AD. As a result, our method for detecting the insidious changes in functional connectivity in Papez circuit could assist in the early detection of MCI and AD risk.

Finally, the possible interactive relationships between the *APOE4* gene and functional connectivity changes in the Papez circuit are of interest. One possible mechanism is related to the cerebral amyloid angiopathy (CAA) that is frequently seen in AD cases and represents one of its histopathological hallmarks. In particular, the capillary CAA is strongly associated with the *APOE4* gene as a risk factor (Attems et al., 2010; Nicoll and McCarron, 2001; Thal et al., 2009). Moreover, the CAA is associated with micro lacuna infarcts of the deep nuclei, such as the caudate and thalamus in patients with autopsy-proven AD (Snowdon et al., 1997). In a mouse model of AD, there is also evidence of CAA and CAA-related capillary occlusion in the thalamic vessels in the branches of the thalamo-perforating arteries (Thal et al., 2009). These results suggest a role of *APOE4* in the microvascular changes commonly found in AD and are consistent with a potential amyloidogenic role for *APOE4* (Yip et al., 2005). Although we remain cautious in advancing our interpretation of the presently observed functional connectivity changes in the Papez circuit, we speculate that the amyloidogenic role for *APOE4* could affect the functional connectivity. Recent studies support this speculation that the amyloid plaques disrupt resting-state connectivity in the default mode network and other cortical hubs in cognitively normal elderly (Drzezga et al., 2011; Hedden et al., 2009; Sheline et al., 2010b). However, another study showed that *APOE4* allele also disrupts resting-state fMRI connectivity in the absence of amyloid plaques (Dennis et al., 2010; Sheline et al., 2010a). Such effects of *APOE4* allele on functional connectivity suggest that these changes may antedate the pathological effects of amyloid plaques. Further study is needed to elucidate the mechanisms.

Supplementary Material

Refer to Web version on PubMed Central for supplementary material.

Acknowledgements

This work was supported by the Extendicare and Birnshein Foundation grant, National Institutes of Health grants R01AG20279 and R44AG035405. The authors thank Ms. Carrie M. O'Connor, MA, for editorial assistance, and Ms. Judi Zaferos-Pylant and Mr. Yu Liu, MS, for MRI technical support.

Author Manuscript Author Manuscript Author Manuscript Author Manuscript

References

Adamson MM, Hutchinson JB, Shelton AL, Wagner AD, Taylor JL. Reduced hippocampal activity during encoding in cognitively normal adults carrying the APOE varepsilon4 allele. Neuropsychologia. 2011; 49(9):2448–2455. [PubMed: 21549723]

Aggleton JP, Brown MW. Episodic memory, amnesia, and the hippocampal-anterior thalamic axis. Behav Brain Sci. 1999; 22(3):425–444. discussion 444-489. [PubMed: 11301518]

Allen G, Barnard H, McColl R, Hester AL, Fields JA, Weiner MF, Ringe WK, Lipton AM, Brooker M, McDonald E, Rubin CD, Cullum CM. Reduced hippocampal functional connectivity in Alzheimer disease. Arch Neurol. 2007; 64(10):1482–1487. [PubMed: 17923631]

Atallah HE, Frank MJ, O'Reilly RC. Hippocampus, cortex, and basal ganglia: insights from computational models of complementary learning systems. Neurobiol Learn Mem. 2004; 82(3): 253–267. [PubMed: 15464408]

Attems J, Yamaguchi H, Saido TC, Thal DR. Capillary CAA and perivascular Abeta-deposition: two distinct features of Alzheimer's disease pathology. J Neurol Sci. 2010; 299(1–2):155–162. [PubMed: 20850138]

Bookheimer SY, Strojwas MH, Cohen MS, Saunders AM, Pericak-Vance MA, Mazziotta JC, Small GW. Patterns of brain activation in people at risk for Alzheimer's disease. N Engl J Med. 2000; 343(7):450–456. [PubMed: 10944562]

Callen DJ, Black SE, Gao F, Caldwell CB, Szalai JP. Beyond the hippocampus: MRI volumetry confirms widespread limbic atrophy in AD. Neurology. 2001; 57(9):1669–1674. [PubMed: 11706109]

Caselli RJ, Dueck AC, Locke DE, Sabbagh MN, Ahern GL, Rapcsak SZ, Baxter LC, Yaari R, Woodruff BK, Hoffman-Snyder C, Rademakers R, Findley S, Reiman EM. Cerebrovascular risk factors and preclinical memory decline in healthy APOE epsilon4 homozygotes. Neurology. 2011; 76(12):1078–1084. [PubMed: 21325652]

Chen G, Ward BD, Xie C, Li W, Wu Z, Jones JL, Franczak M, Antuono P, Li SJ. Classification of Alzheimer disease, mild cognitive impairment, and normal cognitive status with large-scale network analysis based on resting-state functional MR imaging. Radiology. 2011; 259(1):213–221. [PubMed: 21248238]

Corder EH, Saunders AM, Strittmatter WJ, Schmechel DE, Gaskell PC, Small GW, Roses AD, Haines JL, Pericak-Vance MA. Gene dose of apolipoprotein E type 4 allele and the risk of Alzheimer's disease in late onset families. Science. 1993; 261(5123):921–923. [PubMed: 8346443]

Crivello F, Lemaitre H, Dufouil C, Grassiot B, Delcroix N, Tzourio-Mazoyer N, Tzourio C, Mazoyer B. Effects of ApoE-epsilon4 allele load and age on the rates of grey matter and hippocampal volumes loss in a longitudinal cohort of 1186 healthy elderly persons. Neuroimage. 2010; 53(3): 1064–1069. [PubMed: 20060049]

Dennis NA, Browndyke JN, Stokes J, Need A, Burke JR, Welsh-Bohmer KA, Cabeza R. Temporal lobe functional activity and connectivity in young adult APOE varepsilon4 carriers. Alzheimer's & dementia : the journal of the Alzheimer's Association. 2010; 6(4):303–311.

Drzezga A, Becker JA, Van Dijk KR, Sreenivasan A, Talukdar T, Sullivan C, Schultz AP, Sepulcre J, Putcha D, Greve D, Johnson KA, Sperling RA. Neuronal dysfunction and disconnection of cortical hubs in non-demented subjects with elevated amyloid burden. Brain. 2011; 134(Pt 6):1635–1646. [PubMed: 21490054]

Filippini N, MacIntosh BJ, Hough MG, Goodwin GM, Frisoni GB, Smith SM, Matthews PM, Beckmann CF, Mackay CE. Distinct patterns of brain activity in young carriers of the APOE- 4 allele. Proceedings of the National Academy of Sciences of the United States of America. 2009; 106(17):7209–7214. [PubMed: 19357304]

Fleisher AS, Sherzai A, Taylor C, Langbaum JB, Chen K, Buxton RB. Resting-state BOLD networks versus task-associated functional MRI for distinguishing Alzheimer's disease risk groups. Neuroimage. 2009; 47(4):1678–1690. [PubMed: 19539034]

Fox MD, Raichle ME. Spontaneous fluctuations in brain activity observed with functional magnetic resonance imaging. Nat Rev Neurosci. 2007; 8(9):700–711. [PubMed: 17704812]

Author Manuscript Author Manuscript Author Manuscript Author Manuscript

Fox MD, Zhang D, Snyder AZ, Raichle ME. The global signal and observed anticorrelated resting state brain networks. J Neurophysiol. 2009; 101(6):3270–3283. [PubMed: 19339462]

Goveas JS, Xie C, Chen G, Li W, Ward BD, Franczak MB, Jones JL, Antuono PG, Li SJ. Functional network endophenotypes unravel the effects of apolipoprotein E epsilon 4 in middle-aged adults. PLoS One. 2013; 8(2):e55902. [PubMed: 23424640]

Goveas JS, Xie C, Ward BD, Wu Z, Li W, Franczak M, Jones JL, Antuono PG, Li SJ. Recovery of hippocampal network connectivity correlates with cognitive improvement in mild Alzheimer's disease patients treated with donepezil assessed by resting-state fMRI. J Magn Reson Imaging. 2011; 34(4):764–773. [PubMed: 21769962]

Greicius MD, Srivastava G, Reiss AL, Menon V. Default-mode network activity distinguishes Alzheimer's disease from healthy aging: evidence from functional MRI. Proc Natl Acad Sci U S A. 2004; 101(13):4637–4642. [PubMed: 15070770]

Haase L, Wang M, Green E, Murphy C. Functional connectivity during recognition memory in individuals genetically at risk for Alzheimer's disease. Hum Brain Mapp. 2011

Hedden T, Van Dijk KR, Becker JA, Mehta A, Sperling RA, Johnson KA, Buckner RL. Disruption of functional connectivity in clinically normal older adults harboring amyloid burden. J Neurosci. 2009; 29(40):12686–12694. [PubMed: 19812343]

Hornberger M, Wong S, Tan R, Irish M, Piguet O, Kril J, Hodges JR, Halliday G. In vivo and post-mortem memory circuit integrity in frontotemporal dementia and Alzheimer's disease. Brain. 2012; 135(Pt 10):3015–3025. [PubMed: 23012333]

Jacobs DM, Sano M, Dooneief G, Marder K, Bell KL, Stern Y. Neuropsychological detection and characterization of preclinical Alzheimer's disease. Neurology. 1995; 45(5):957–962. [PubMed: 7746414]

Jicha GA, Carr SA. Conceptual evolution in Alzheimer's disease: implications for understanding the clinical phenotype of progressive neurodegenerative disease. J Alzheimers Dis. 2010; 19(1):253–272. [PubMed: 20061643]

Jones BF, Barnes J, Uylings HB, Fox NC, Frost C, Witter MP, Scheltens P. Differential regional atrophy of the cingulate gyrus in Alzheimer disease: a volumetric MRI study. Cereb Cortex. 2006; 16(12):1701–1708. [PubMed: 16400164]

Konrad C, Ukas T, Nebel C, Arolt V, Toga AW, Narr KL. Defining the human hippocampus in cerebral magnetic resonance images--an overview of current segmentation protocols. Neuroimage. 2009; 47(4):1185–1195. [PubMed: 19447182]

Li SJ, Li Z, Wu G, Zhang MJ, Franczak M, Antuono PG. Alzheimer Disease: evaluation of a functional MR imaging index as a marker. Radiology. 2002; 225(1):253–259. [PubMed: 12355013]

Lind J, Persson J, Ingvar M, Larsson A, Cruts M, Van Broeckhoven C, Adolfsson R, Backman L, Nilsson LG, Petersson KM, Nyberg L. Reduced functional brain activity response in cognitively intact apolipoprotein E epsilon4 carriers. Brain. 2006; 129(Pt 5):1240–1248. [PubMed: 16537568]

Machulda MM, Jones DT, Vemuri P, McDade E, Avula R, Przybelski S, Boeve BF, Knopman DS, Petersen RC, Jack CR Jr. Effect of APOE epsilon4 status on intrinsic network connectivity in cognitively normal elderly subjects. Arch Neurol. 2011; 68(9):1131–1136. [PubMed: 21555604]

Machulda MM, Senjem ML, Weigand SD, Smith GE, Ivnik RJ, Boeve BF, Knopman DS, Petersen RC, Jack CR. Functional magnetic resonance imaging changes in amnestic and nonamnestic mild cognitive impairment during encoding and recognition tasks. J Int Neuropsychol Soc. 2009; 15(3): 372–382. [PubMed: 19402923]

Madsen SK, Ho AJ, Hua X, Saharan PS, Toga AW, Jack CR Jr, Weiner MW, Thompson PM. 3D maps localize caudate nucleus atrophy in 400 Alzheimer's disease, mild cognitive impairment, and healthy elderly subjects. Neurobiol Aging. 2010; 31(8):1312–1325. [PubMed: 20538376]

Mayeux R, Saunders AM, Shea S, Mirra S, Evans D, Roses AD, Hyman BT, Crain B, Tang MX, Phelps CH. Utility of the apolipoprotein E genotype in the diagnosis of Alzheimer's disease. Alzheimer's Disease Centers Consortium on Apolipoprotein E and Alzheimer's Disease. N Engl J Med. 1998; 338(8):506–511. [PubMed: 9468467]

Mechelli A, Price CJ, Friston KJ, Ashburner J. Voxel-based morphometry of the human brain: Methods and applications. Current Medical Imaging Reviews. 2005; 1(2):105–113.

Author Manuscript Author Manuscript Author Manuscript Author Manuscript

Meyer MR, Tschanz JT, Norton MC, Welsh-Bohmer KA, Steffens DC, Wyse BW, Breitner JC. APOE genotype predicts when--not whether--one is predisposed to develop Alzheimer disease. Nat Genet. 1998; 19(4):321–322. [PubMed: 9697689]

Nicoll JA, McCarron MO. APOE gene polymorphism as a risk factor for cerebral amyloid angiopathy-related hemorrhage. Amyloid : the international journal of experimental and clinical investigation : the official journal of the International Society of Amyloidosis. 2001; 8(Suppl 1):51–55.

Papez JW. A proposed mechanism of emotion. Arch Neurol Psychiatry. 1937; 38(4):725–743.

Pievani M, Galluzzi S, Thompson PM, Rasser PE, Bonetti M, Frisoni GB. APOE4 is associated with greater atrophy of the hippocampal formation in Alzheimer's disease. Neuroimage. 2011; 55(3): 909–919. [PubMed: 21224004]

Reiter K, Alpert KI, Cobia DJ, Kwasny MJ, Morris JC, Csernansky JC, Wang L. Cognitively normal individuals with AD parents may be at risk for developing aging-related cortical thinning patterns characteristic of AD. Neuroimage. 2012; 61(3):525–532. [PubMed: 22503937]

Rombouts SA, Stam CJ, Kuijer JP, Scheltens P, Barkhof F. Identifying confounds to increase specificity during a "no task condition". Evidence for hippocampal connectivity using fMRI. Neuroimage. 2003; 20(2):1236–1245. [PubMed: 14568492]

Ryan NS, Keihaninejad S, Shakespeare TJ, Lehmann M, Crutch SJ, Malone IB, Thornton JS, Mancini L, Hyare H, Yousry T, Ridgway GR, Zhang H, Modat M, Alexander DC, Rossor MN, Ourselin S, Fox NC. Magnetic resonance imaging evidence for presymptomatic change in thalamus and caudate in familial Alzheimer's disease. Brain. 2013; 136(Pt 5):1399–1414. [PubMed: 23539189]

Scarmeas N, Stern Y. Imaging studies and APOE genotype in persons at risk for Alzheimer's disease. Current psychiatry reports. 2006; 8(1):11–17. [PubMed: 16513038]

Sheline YI, Morris JC, Snyder AZ, Price JL, Yan Z, D'Angelo G, Liu C, Dixit S, Benzinger T, Fagan A, Goate A, Mintun MA. APOE4 allele disrupts resting state fMRI connectivity in the absence of amyloid plaques or decreased CSF Abeta42. J Neurosci. 2010a; 30(50):17035–17040. [PubMed: 21159973]

Sheline YI, Raichle ME, Snyder AZ, Morris JC, Head D, Wang S, Mintun MA. Amyloid plaques disrupt resting state default mode network connectivity in cognitively normal elderly. Biol Psychiatry. 2010b; 67(6):584–587. [PubMed: 19833321]

Small GW, Ercoli LM, Silverman DH, Huang SC, Komo S, Bookheimer SY, Lavretsky H, Miller K, Siddarth P, Rasgon NL, Mazziotta JC, Saxena S, Wu HM, Mega MS, Cummings JL, Saunders AM, Pericak-Vance MA, Roses AD, Barrio JR, Phelps ME. Cerebral metabolic and cognitive decline in persons at genetic risk for Alzheimer's disease. Proc Natl Acad Sci U S A. 2000; 97(11): 6037–6042. [PubMed: 10811879]

Smith AD. Imaging the progression of Alzheimer pathology through the brain. Proceedings of the National Academy of Sciences of the United States of America. 2002; 99(7):4135–4137. [PubMed: 11929987]

Snowdon DA, Greiner LH, Mortimer JA, Riley KP, Greiner PA, Markesbery WR. Brain infarction and the clinical expression of Alzheimer disease. The Nun Study. JAMA. 1997; 277(10):813–817. [PubMed: 9052711]

Thal DR, Capetillo-Zarate E, Larionov S, Staufenbiel M, Zurbruegg S, Beckmann N. Capillary cerebral amyloid angiopathy is associated with vessel occlusion and cerebral blood flow disturbances. Neurobiol Aging. 2009; 30(12):1936–1948. [PubMed: 18359131]

Verghese PB, Castellano JM, Holtzman DM. Apolipoprotein E in Alzheimer's disease and other neurological disorders. Lancet neurology. 2011; 10(3):241–252.

Villain N, Desgranges B, Viader F, de la Sayette V, Mezenge F, Landeau B, Baron JC, Eustache F, Chetelat G. Relationships between hippocampal atrophy, white matter disruption, and gray matter hypometabolism in Alzheimer's disease. J Neurosci. 2008; 28(24):6174–6181. [PubMed: 18550759]

Vincent JL, Kahn I, Snyder AZ, Raichle ME, Buckner RL. Evidence for a frontoparietal control system revealed by intrinsic functional connectivity. J Neurophysiol. 2008; 100(6):3328–3342. [PubMed: 18799601]

Author Manuscript Author Manuscript Author Manuscript Author Manuscript

Vincent JL, Snyder AZ, Fox MD, Shannon BJ, Andrews JR, Raichle ME, Buckner RL. Coherent spontaneous activity identifies a hippocampal-parietal memory network. J Neurophysiol. 2006; 96(6):3517–3531. [PubMed: 16899645]

Wang L, Zang Y, He Y, Liang M, Zhang X, Tian L, Wu T, Jiang T, Li K. Changes in hippocampal connectivity in the early stages of Alzheimer's disease: evidence from resting state fMRI. Neuroimage. 2006; 31(2):496–504. [PubMed: 16473024]

Welsh K, Butters N, Hughes J, Mohs R, Heyman A. Detection of abnormal memory decline in mild cases of Alzheimer's disease using CERAD neuropsychological measures. Arch Neurol. 1991; 48(3):278–281. [PubMed: 2001185]

Westlye ET, Lundervold A, Rootwelt H, Lundervold AJ, Westlye LT. Increased hippocampal default mode synchronization during rest in middle-aged and elderly APOE epsilon4 carriers: relationships with memory performance. J Neurosci. 2011; 31(21):7775–7783. [PubMed: 21613490]

Xu Y, Xu G, Wu G, Antuono P, Rowe DB, Li SJ. The phase shift index for marking functional asynchrony in Alzheimer's disease patients using fMRI. Magn Reson Imaging. 2008; 26(3):379–392. [PubMed: 18164158]

Yip AG, McKee AC, Green RC, Wells J, Young H, Cupples LA, Farrer LA. APOE, vascular pathology, and the AD brain. Neurology. 2005; 65(2):259–265. [PubMed: 16043796]

Zarei M, Patenaude B, Damoiseaux J, Morgese C, Smith S, Matthews PM, Barkhof F, Rombouts SA, Sanz-Arigita E, Jenkinson M. Combining shape and connectivity analysis: an MRI study of thalamic degeneration in Alzheimer's disease. Neuroimage. 2010; 49(1):1–8. [PubMed: 19744568]

Author Manuscript Author Manuscript Author Manuscript Author Manuscript

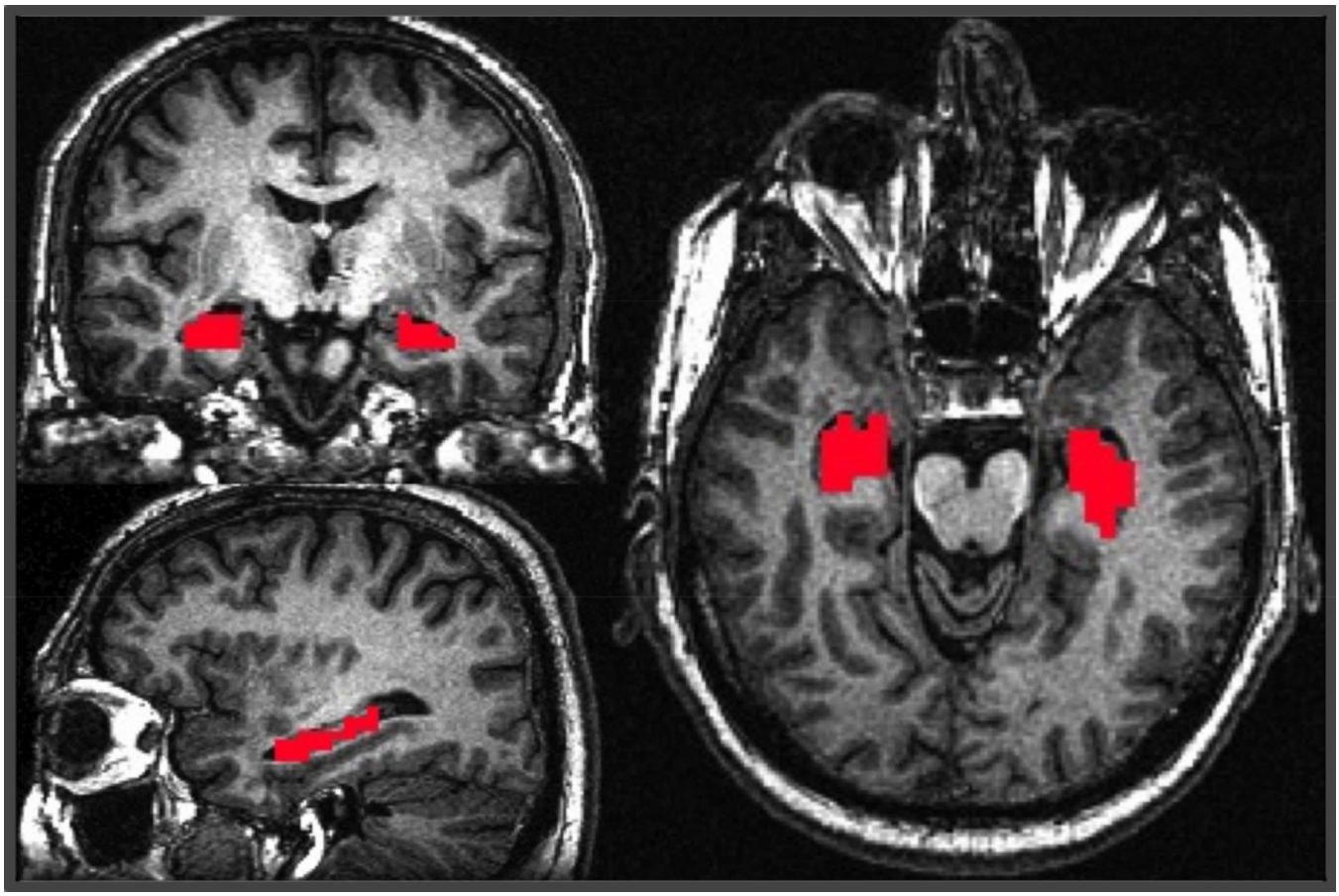

Figure 1.
A representative view of the hippocampus as the seed region from a subject. The seed was manually traced (red voxels) in the T1-weighted high-resolution anatomical image.

Author Manuscript Author Manuscript Author Manuscript Author Manuscript

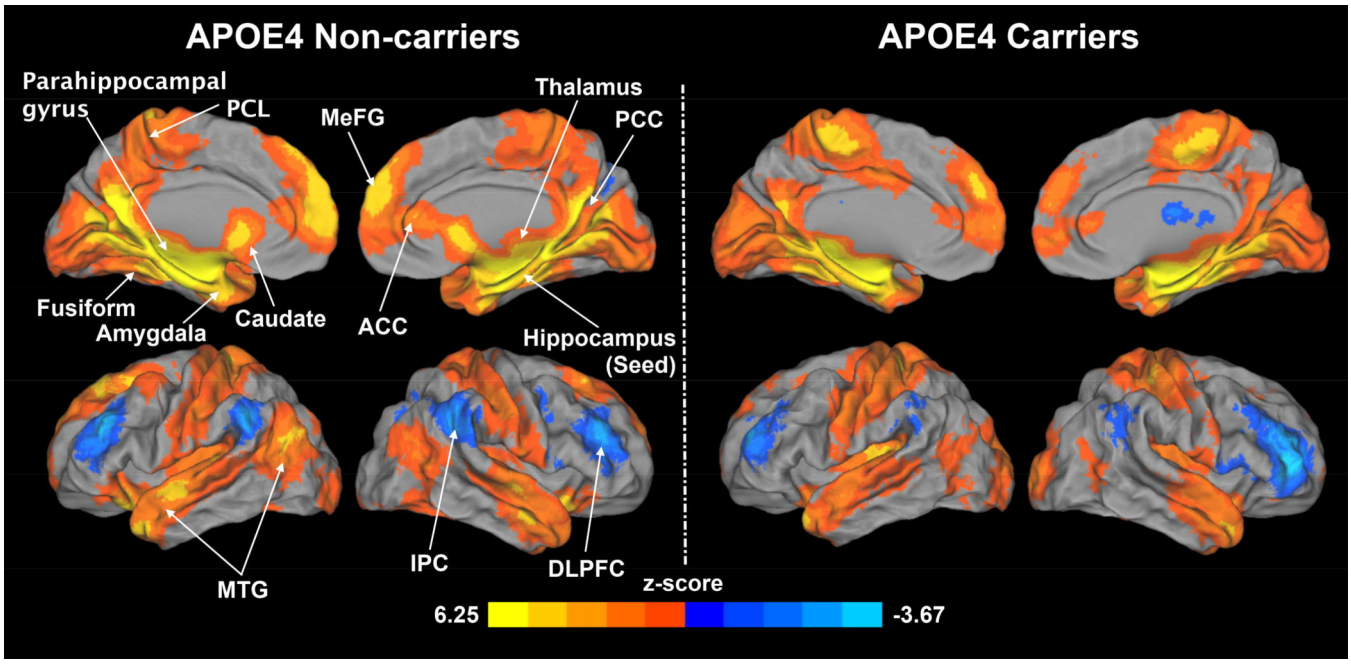

Figure 2.

Patterns of the hippocampus functional connectivity (HFC) for *APOE4* noncarriers (left) and carriers (right). Warm colors and cool colors indicate positive and negative functional connectivity, respectively. DLPFC: dorsal lateral prefrontal cortex, IPC: inferior parietal cortex, MTG: middle temporal gyrus, ACC: anterior cingulate cortex, PCC: posterior cingulate cortex, MeFG: medial frontal gyrus, PCL: paracentral lobule.

Author Manuscript Author Manuscript Author Manuscript Author Manuscript

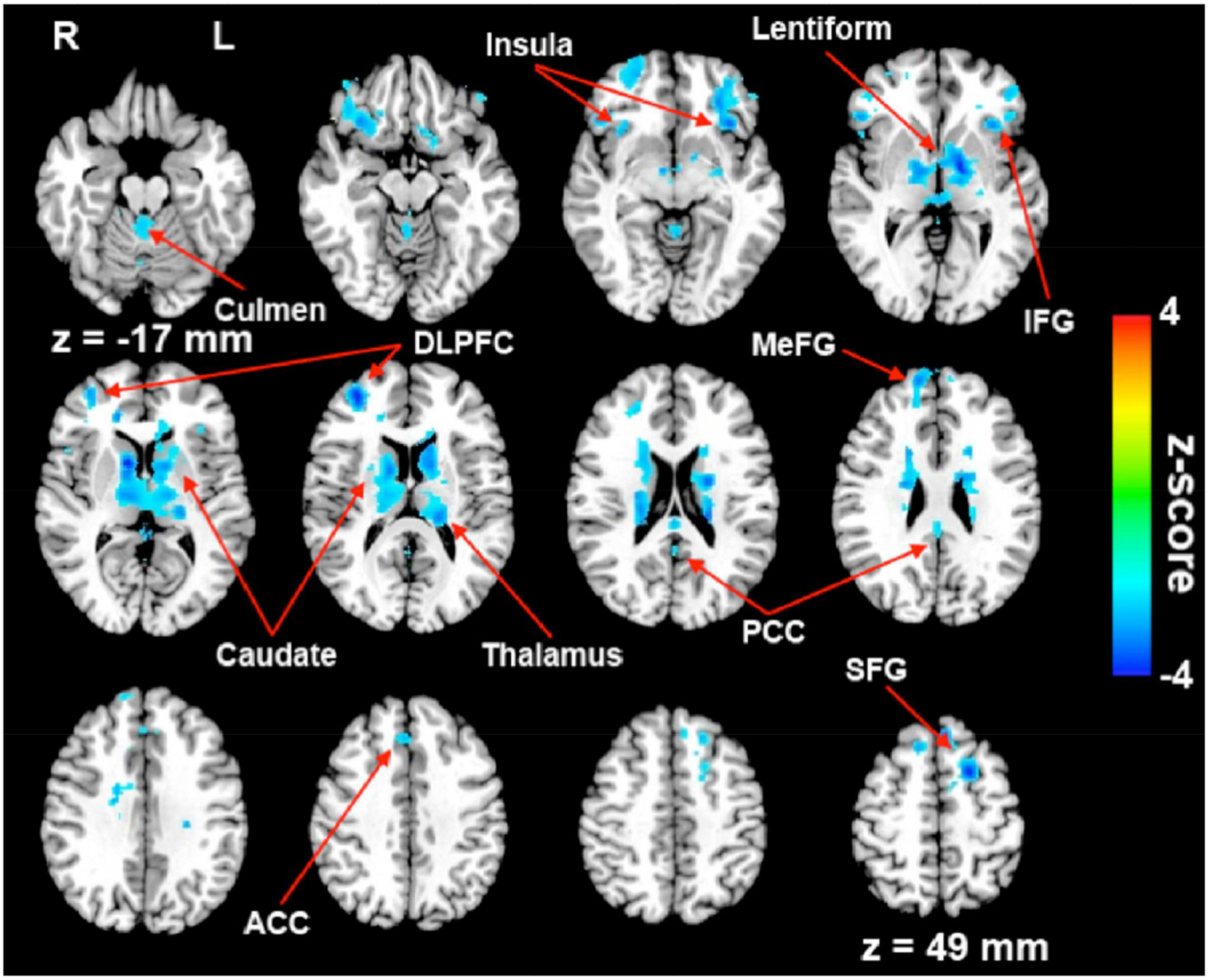

Figure 3.

Patterns of decreased HFC in *APOE4* carriers compared with noncarriers. Cool colors indicate decreased HFC in *APOE4* carriers. DLPFC: dorsal lateral prefrontal cortex; MeFG: medial frontal gyrus; SFG: superior frontal gyrus, IFG: inferior frontal gyrus, ACC: anterior cingulate gyrus, PCC: posterior cingulate gyrus.

Author Manuscript Author Manuscript Author Manuscript Author Manuscript

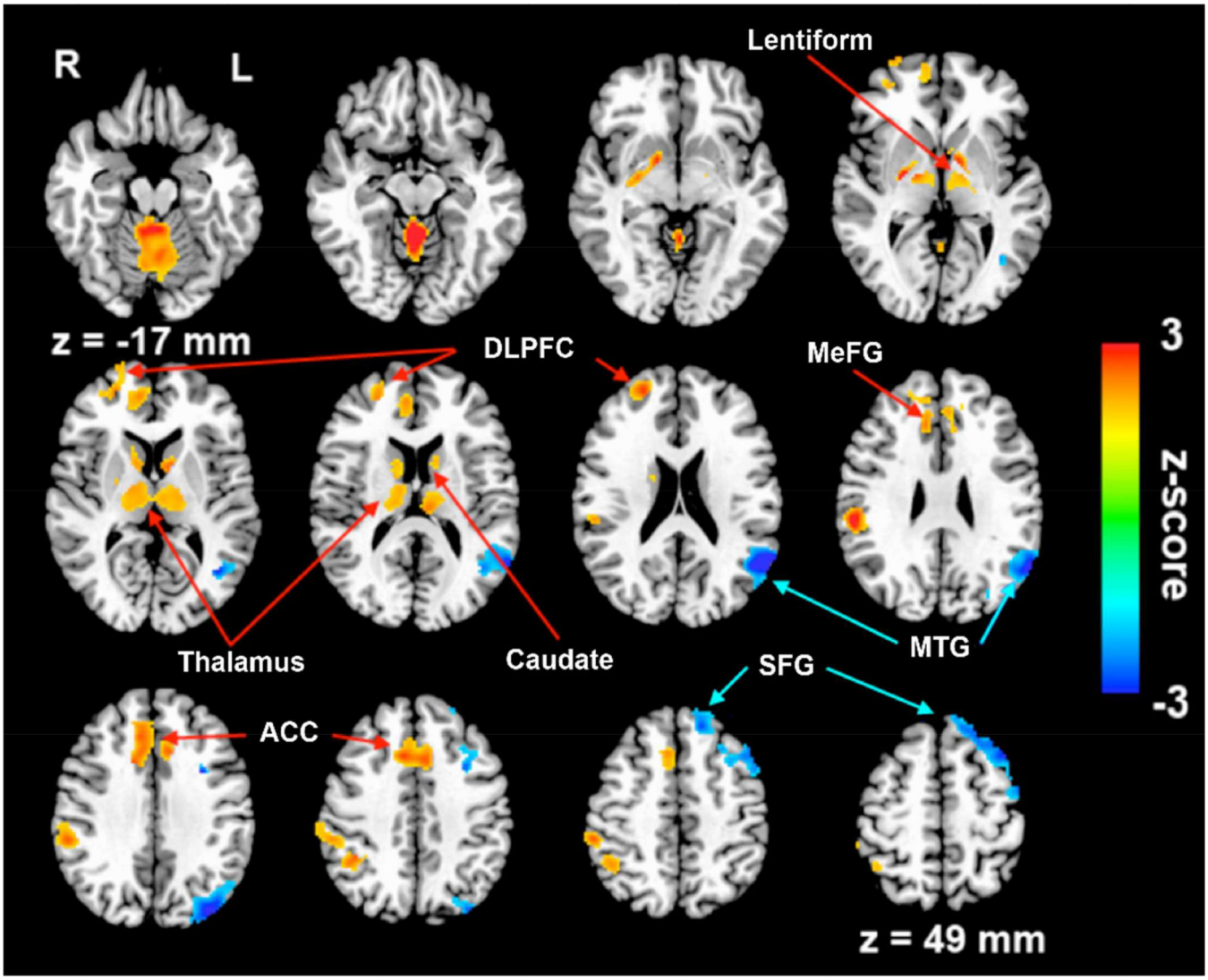

Figure 4.

The neural correlates of RAVLT delayed recall scores. Brain regions with positive correlation are indicated by red arrows. Those with negative correlation are indicated by blue arrows. DLPFC: dorsal lateral prefrontal cortex, MeFG: medial frontal gyrus, ACC: anterior cingulate gyrus, SFG: superior frontal gyrus, MTG: middle temporal gyrus.

Author Manuscript Author Manuscript Author Manuscript Author Manuscript

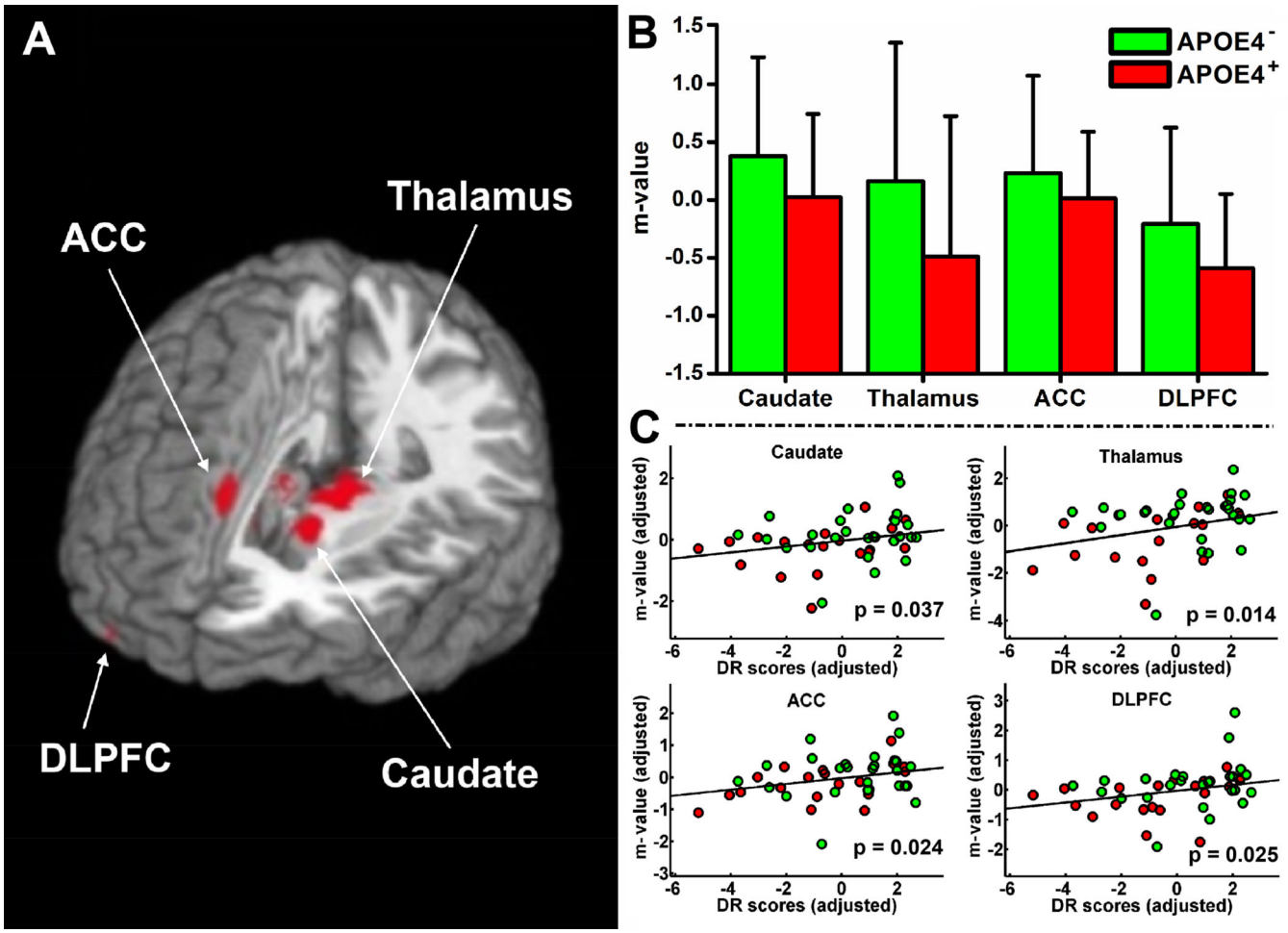

Figure 5.

(A) Conjunction between the brain regions with HFC changes and the neural correlates of episodic memory function. (B) Numerical presentation of the overlapping brain regions (colored red) between the neural correlates of memory function and the decreased HFC. The *m*-value in the *y*-axis indicates the Fisher-transformed HFC and error bars indicate the standard deviations. (C) Representative correlations between HFC and the RAVLT-DR scores from the overlapping brain regions. APOE4-: APOE4 noncarriers, APOE4+: APOE4 carriers, DLPFC: dorsal lateral prefrontal cortex, ACC: anterior cingulate gyrus. RAVLT-DR: Rey auditory verbal learning test for delayed recall.

Author Manuscript Author Manuscript Author Manuscript Author Manuscript

Table 1

Demographic Characteristics

	APOE4 carriers n = 20	*APOE4* noncarriers n = 26	*p*-value
	Mean ± SD	**Mean ± SD**	
Gender, female/male	14/6	17/9	NS
Age, year	52.4 ± 5.6	54.5 ± 5.8	0.21
Education, year	15.0 ± 2.4	15.6 ± 2.5	0.86
RAVLT total learn	49.5 ± 6.2	59.7 ± 7.6	0.15
RAVLT-DR	12.1 ± 2.2	13.1 ± 1.9	0.10
Digital Span	16.6 ± 3.6	18.5 ± 3.4	0.07
Trail-making test			
A	24.2 ± 8.3	23.5 ± 8.7	0.81
B	56.0 ± 19.4	50.2 ± 18.7	0.31

NS: no significant difference by χ^2 test between groups, RAVLT: Rey Auditory Verbal Learning Test, DR: delayed recall.

Author Manuscript Author Manuscript Author Manuscript Author Manuscript

Table 2

Significant Decreased HFC in *APOE4* Carriers Compared with Noncarriers

Side	Brain region	BA	Cluster size (mm^3)	Talairach coordinates (LPI)			z-score
				x	y	z	
R	Caudate		41990	10	5	8	4.34
L	Caudate			−12	5	11	3.12
R	Thalamus			11	−9	−1	3.27
L	Thalamus			−19	−28	16	3.37
L	Lentiform nucleus			−14	−6	1	3.77
L	PCC	30		−1	−48	16	2.28
R	PCC	30		3	−49	14	2.46
R	Culmen			2	−41	−21	2.71
L	Culmen			−1	−44	−21	2.97
R	DLPFC	10	7129	33	48	12	3.60
R	ACC	32		16	36	9	3.27
R	SFG	6, 9		10	56	26	3.12
R	IFG	47		31	20	−10	2.96
L	MeFG	6	6255	−20	7	50	3.65
L	SFG	8		−5	31	50	3.37
L	IFG	47		−33	21	−3	3.43
L	Insula	13		−34	20	2	2.88

Note: BA: brodmann area, PCC: posterior cingulate cortex, ACC: anterior cingulated cortex, DLPFC: dorsolateral prefrontal cortex, MeFG: medial frontal gyrus, SFG: superior frontal gyrus, IFG: inferior frontal gyrus.

Cortex. Author manuscript; available in PMC 2015 August 01.